Published in final edited form as:
Hepatology. 2014 July ; 60(1): 311–322. doi:10.1002/hep.27035.

Mesodermal mesenchymal cells give rise to myofibroblasts, but not epithelial cells, in mouse liver injury

Ingrid Lua[1], **David James**[2], **Jiaohong Wang**[1], **Kasper S. Wang**[2], and **Kinji Asahina**[1]

[1]Southern California Research Center for ALPD and Cirrhosis, Department of Pathology, Keck School of Medicine, University of Southern California

[2]Saban Research Institute, Children's Hospital Los Angeles

Abstract

Hepatic stellate cells (HSCs) and portal fibroblasts (PFs) are believed to be the major source of myofibroblasts that participate in fibrogenesis via synthesis of proinflammatory cytokines and extracellular matrices. Previous lineage tracing studies using MesP1^{Cre} and Rosa26lacZ^{flox} mice demonstrated that MesP1+ mesoderm gives rise to mesothelial cells (MCs), which differentiate into HSCs and PFs during liver development. In contrast, several in vivo and in vitro studies reported that HSCs can differentiate into other cell types, including hepatocytes, cholangiocytes, and progenitor cell types known as oval cells, thereby acting as stem cells in the liver. To test whether HSCs give rise to epithelial cells in adult liver, we determined the hepatic lineages of HSCs and PFs using MesP1^{Cre} and Rosa26mTmG^{flox} mice. Genetic cell lineage tracing revealed that the MesP1+ mesoderm gives rise to MCs, HSCs, and PFs, but not to hepatocytes or cholangiocytes, in the adult liver. Upon carbon tetrachloride injection or bile duct ligation surgery-mediated liver injury, mesodermal mesenchymal cells, including HSCs and PFs, differentiate into myofibroblasts but not into hepatocytes or cholangiocytes. Furthermore, differentiation of the mesodermal mesenchymal cells into oval cells was not observed. These results indicate that HSCs are not sufficiently multipotent to produce hepatocytes, cholangiocytes, or oval cells via mesenchymal-epithelial transition in vivo. In conclusion, cell lineage tracing demonstrated that mesodermal mesenchymal cells including HSCs are the major source of myofibroblasts but do not differentiate into epithelial cell types such as hepatocytes, cholangiocytes, and oval cells.

Keywords

Fibrosis; Hepatic stellate cells; Mesenchymal-epithelial transition; Oval cells; Portal fibroblasts

Introduction

Liver fibrosis is a scarring process caused by chronic insults such as alcohol consumption, hepatitis viral infection, and obesity.[1–4] Upon liver injury, hepatic stellate cells (HSCs) residing in the space of Disse are activated and differentiate into myofibroblastic cells,

Contact information. Address reprint requests to: Kinji Asahina, Ph.D., Southern California Research Center for ALPD and Cirrhosis, Department of Pathology, Keck School of Medicine, University of Southern California, 1333 San Pablo St., MMR 301, Los Angeles, CA 90033-9141, Tel: 323-442-2213, Fax: 323-442-3126, asahina@usc.edu.

which synthesize proinflammatory cytokines and extracellular matrices and induce fibrosis via the deposition of collagen fibers.[5,6] Myofibroblasts in the injured liver also contribute to cancer progression and metastasis.[7] Although HSCs are considered a major source of fibrotic myofibroblasts, portal fibroblasts (PFs) adjacent to the bile duct in the Glisson's capsule also yield myofibroblasts in biliary fibrosis.[8] Furthermore, mesothelial cells (MCs) covering the liver surface have been shown to differentiate into myofibroblasts during fibrogenesis.[9] Even though multiple cell types, including HSCs, PFs, and MCs, are believed to represent the source of myofibroblasts in liver injury, genetic cell lineage tracing studies using Mesoderm posterior 1 (MesP1)^{Cre} and Rosa26lacZ^{flox} mice demonstrated that all of these cells are mesodermal in origin in liver development.[10,11] Lineage tracing further revealed that MCs act as mesenchymal progenitor cells and produce HSCs, fibroblasts around veins, and smooth muscle cells (SMCs) in embryonic liver. These studies indicate that the liver mesenchymal cell lineage is distinct from liver epithelial cell lineages, such as hepatocytes and cholangiocytes, which arise from definitive endoderm. Although hepatocytes or cholangiocytes were thought to differentiate into myofibroblasts via an epithelial-mesenchymal transition (EMT),[12–14] this notion was refuted by cell lineage tracing with different Cre mouse lines.[15,16]

During liver development, definitive endoderm gives rise to hepatoblasts, which are bi-potent progenitor cells that give rise to hepatocytes and cholangiocytes.[17] Hepatoblasts form the ductal plate adjacent to the portal vein and differentiate into cholangiocytes, which subsequently form the bile duct in adults.[18] In the adult liver, mature hepatocytes have enormous regeneration potential. Following partial hepatectomy, hepatocytes initiate DNA synthesis and compensate for the loss of liver lobes without contribution from stem cells. Interestingly, when the proliferative potential of hepatocytes is impaired, facultative hepatic progenitor cells (also known as oval cells) emerge in the portal area.[19–22] Oval cells are epithelial cells with ovoid nuclei and minimal cytoplasm that express cholangiocyte markers such as cytokeratin 19 (CK19), SOX9, EPCAM, and osteopontin.[18,23,24] A morphological study suggested that oval cells arise from the Canals of Hering, a connection between hepatocytes and cholangiocytes, and give rise to these cell types during regeneration in a manner comparable to the differentiation pathway of embryonic hepatoblasts.[25] Cell lineage tracing with Sox9^{CreERT2} mice demonstrated that oval cells arise from the SOX9+ ductal plate.[18] Furthermore, osteopontin+ cholangiocytes were shown to be the origin of oval cells.[24]

Even though numerous studies using different Cre mouse lines have demonstrated that liver epithelial cells and mesenchymal cells are endodermal and mesodermal in origin, respectively, the differentiation of HSCs into oval cells via mesenchymal-epithelial transition (MET) was also reported following cell lineage tracing with glial fibrillary acidic protein (GFAP)^{Cre} and α-smooth muscle actin (ACTA2)^{CreERT2} mice.[26,27] In addition, cell culture studies have demonstrated the multi-differentiation potential of HSCs. Kordes et al. reported that promin 1/CD133 (PROM1)+ HSCs isolated from rat liver can differentiate into myofibroblasts, endothelial cells, or hepatocytes under different culture conditions.[28] Conigliaro et al. showed that mouse liver stem cell lines have the potential to differentiate into both epithelial and mesenchymal lineages in culture.[29] Although our group previously demonstrated that HSCs are derived from MesP1+ mesoderm in liver development,[10] it

remained to be seen whether the progeny of mesodermal HSCs are capable of differentiating into endodermal epithelial cells in injured adult livers. Thus, the present study extended our previous lineage tracing using the $MesP1^{Cre}$ mouse to determine the fate of liver mesenchymal cells in the adult liver. We found that MesP1+ mesoderm gives rise to HSCs, PFs, and SMCs, but not hepatocytes and cholangiocytes, in the adult liver. After induction of fibrosis by CCl_4 injection or bile duct ligation (BDL), mesodermal liver mesenchymal cells, including HSCs and PFs, differentiated into myofibroblasts but not into liver epithelial cells. Furthermore, the mesodermal mesenchymal cells did not give rise to oval cells induced with a 3,5-diethoxycarbonyl-1,4-dihydrocollidine (DDC) diet. The present study demonstrates that mesodermal mesenchymal cells are the primary source of myofibroblasts and do not give rise to epithelial cells types such as hepatocytes, cholangiocytes, and oval cells.

Materials and methods

Mice

$MesP1^{Cre}$, $Rosa26mTmG^{flox}$ ($R26T/G^{f}$) mice were described previously.[30,31] Male $MesP1^{Cre/+}$;$R26TG^{f/f}$ mice were used for experiments. Fibrosis was induced by subcutaneous injection of CCl_4 (1 ml/kg body weight, 3 mice) with mineral oil in a 1:3 dilution every third day for a total of 30 injections.[9] To induce biliary fibrosis, the mice were subjected to BDL for 2 weeks (3 mice).[9] For oval cell induction, 5 mice were fed 0.1% DDC chow and were sacrificed 3 mice at 4 weeks.[32] The remaining 2 mice were additionally fed normal chow for 4 weeks. $MesP1^{+/+}$;$R26TG^{f/f}$ mice were used for negative controls. The mice were handled in accordance with protocols approved by the Institutional Animal Care and Use Committee of the University of Southern California.

Immunohistochemistry

Tissues were fixed with 4% paraformaldehyde in PBS or 70% ethanol for 4 h and incubated with 15% sucrose in PBS for 4 h at 4 °C. After incubating with 30% sucrose in PBS overnight, tissues were cryo-embedded in OCT compound (Sakura Finetech, Torrance, CA). Sections were cut at a thickness of 7 μm in a cryostat (CM1900; Leica, Buffalo Grove, IL). For immunostaining with antibodies against A6,[33] tissues were embedded without fixation and cryosections were post-fixed with 70% ethanol. For the immunostaining of R26T/G tissues, TOMATO fluorescence was bleached with 3% H_2O_2 in methanol for 30 min. After blocking with 5% serum, the sections were incubated with the primary antibodies for 1 h at room temperature. The primary antibodies were detected with secondary antibodies conjugated with fluorescent dyes by incubation for 30 min. The antibodies used in immunostaining are listed in Supporting Table 1. The sections were counterstained with DAPI and were observed under a fluorescence microscope (90i; Nikon, Melville, NY). To quantify green fluorescence protein (GFP) expression, at least 3 sections were immunostained for each mouse. Digital images were captured using a 40× objective (at least 15 images per animal) and more than 1,000 cells were counted for each antigen.

Isolation and culture of HSCs

HSCs were isolated by the Non-Parenchymal Liver Cell Core of the Southern California Research Center for ALPD and Cirrhosis (R24AA012885).[9] The mouse liver was perfused via superior vena cava first with EMEM at 5 mL/min for 10 min, then with 0.7% (wt/vol) pronase for 20 min, and finally with 0.044% (wt/vol) collagenase for 10 min. After agitation of the digested liver tissue with 10 μg/mL DNase in a rotary shaker for 15 min, the cell suspension was centrifuged at 50 ×*g* for 30 s, and the supernatant was then centrifuged at 150 ×*g* for 5 min. After twice washing the pellet after centrifugation at 150 ×*g*, the cells were laid on the top of four OptiPrep gradients (1.085, 1.058, 1.043, and 1.034; Sigma-Aldrich, St. Louis, MO) in Beckman ultracentrifuge tubes (Beckman Coulter, Brea, CA). The tubes were centrifuged in the SW-41Ti rotor at 20,000 rpm for 15 min at 25 °C. A pure HSC fraction was collected from the medium/1.035/1.043 interfaces and was either subjected to fluorescence-activated cell sorting (FACS) or cultured in DMEM containing 10% FBS.

FACS

HSCs were subjected to FACS using a FACS Aria sorter (BD Bioscience, San Jose, CA) in the USC Flow Cytometry Core, which is supported by the NCI award (P30CA014089). GFP was detected by an argon laser and a 530 nm filter. Autofluorescence of vitamin A (VitA) was analyzed with a krypton laser and a 424 nm filter. Cells were sorted based on the intensities of GFP and vitamin A autofluorescence.

Immunocytochemistry

Cultured HSCs were fixed with 4% paraformaldehyde in PBS for 10 min at 4 °C. After bleaching TOMATO fluorescence, the cells were blocked with 5% serum for 30 min and incubated with primary antibodies for 1 h at room temperature. The primary antibodies were detected with secondary antibodies conjugated to fluorescent dyes. The antibodies used in immunostaining are listed in Supporting Table 1. The signals were captured with a fluorescent microscope (Axio Observer; Carl Zeiss, Thornwood, NY) equipped with a digital camera (AxioCam; Carl Zeiss).

Quantitative Polymerase Chain Reaction (QPCR)

Total RNA was extracted with RNAqueous Micro (Life Technologies, Carlsbad, CA) and cDNA was synthesized using SuperScript III (Life Technologies).[9] QPCR was performed with SYBR Green in ViiA7 Real-Time PCR System (Applied Biosystems, Foster City, CA). Primer sequences are listed in Supporting Table 2. The samples were run in triplicate. The relative mRNA levels per samples were calculated by subtracting the detection limit (40 Ct) from the cycle threshold value (Ct) of each gene in the same sample to obtain the ΔCt value. Taking the log2 of −ΔCt resulted in the relative expression value of each gene for each sample expressed in arbitrary units. Each value was normalized against Gapdh.

Results

MesP1^{+} mesoderm gives rise to HSCs, PFs, SMCs, and MCs in the adult liver

MesP1 is a basic helix-loop-helix transcription factor transiently expressed in early mesoderm during mouse gastrulation.[30] The MesP1^{Cre} mouse has been used for tracing a mesodermal lineage in the developing heart. We previously demonstrated that liver mesenchymal cells, including HSCs, fibroblasts around the vein, and SMCs in the portal vein, are derived from MesP1+ mesoderm in embryonic livers using the MesP1^{Cre} and Rosa26lacZ^{flox} mice.[10,11] However, it remained to be determined whether these mesodermal mesenchymal cells are the source of myofibroblasts in liver fibrosis. Furthermore, recent studies raised the possibility that HSCs undergo MET and give rise to hepatocytes and oval cells in injured livers.[26,27] Thus, the present study was undertaken to trace cell lineages of the MesP1+ mesoderm-derived mesenchymal cells in the adult liver using MesP1^{Cre} and Rosa26mTmG^{flox} (R26T/G^{flox}) reporter mice. Upon recombination by Cre, the R26T/G^{flox} mouse switches from expression of membrane-tagged TOMATO to GFP (Fig. 1A).[31] The membrane-bound GFP enabled us to observe cell morphology and unequivocally identify GFP-expressing cells in the tissues. In the normal MesP1$^{Cre/+}$;R26T/G$^{f/f}$ adult liver, TOMATO was expressed on the membrane of hepatocytes that could be distinguished by their large round nuclei (Fig. 1B). GFP was expressed in cells in the sinusoid but not in hepatocytes (Fig. 1B). After quenching TOMATO fluorescence with methanol, we characterized GFP expressing cells via immunohistochemistry. As shown in Fig. 1C, many DESMIN (DES)+ HSCs expressed GFP in the sinusoid (80.9±3.1%, 1,656 DES+ HSCs examined, n=3 mice). MCs, which act as progenitor cells for HSCs,[9,11] expressed GFP on the liver surface (Fig. 1C). Podoplanin (PDPN), a mucin-type transmembrane glycoprotein, is expressed in MCs, the lumen of the bile duct, and lymphatic vessel in the mouse liver.[9] We confirmed the specific expression of GFP in PDPN+ MCs (Fig. 1D). GFP expression was also observed in DES+ fibroblasts in the connective tissue around the portal vein and bile duct (Fig. 1C). Deposition of Elastin (ELN), a marker for PFs,[34] was observed around the GFP+ fibroblasts (Fig. 1E), indicating mesodermal origin of PFs. GFP was also expressed in ACTA2+ SMCs of the portal vein and hepatic artery (Fig. 1C,F). In addition, endothelial cells in the portal vein and hepatic artery expressed GFP (Fig. 1 C,F). As expected, no GFP expression was observed in E-cadherin (CDH1)+ HNF4+ hepatocytes and CDH1+ CK19+ cholangiocytes in the liver (Fig. 1G–I). PDPN+ bile duct and lymphatic endothelial cells were negative for GFP (Supporting Fig. 1A). Expression of GFP and CD31, a marker for endothelial cells, or CD45, a leukocyte marker, demonstrated only minimal overlap in the sinusoid (Supporting Fig. 1B,C). A few F4/80+ Kupffer cells were positive for GFP (Supporting Fig. 1D). The control MesP1$^{+/+}$;R26T/G$^{f/f}$ liver did not show GFP expression (Supporting Fig. 1E,F). Cell lineage tracing demonstrated that MesP1+ mesoderm gives rise to MCs and mesenchymal cells, including HSCs, PFs, and SMCs, but not epithelial cells, such as hepatocytes and cholangiocytes, in the adult mouse liver.

Mesodermal origin of HSCs

To validate specific expression of GFP in HSCs, we isolated HSCs from the normal MesP1$^{Cre/+}$ or MesP1^{++};R26T/G$^{f/f}$ adult livers via collagenase perfusion and subsequent discontinuous gradient centrifugation. In culture, primary HSCs isolated from the

MesP1$^{Cre/+}$;R26T/G$^{f/f}$ mouse showed mutually exclusive expression of TOMATO and GFP, which indicated no de novo Cre activation in HSCs (Fig. 2A). The control HSCs isolated from the MesP1$^{+/+}$;R26T/G$^{f/f}$ liver did not show GFP expression (Fig. 2A). After quenching TOMATO fluorescence, the HSCs were immunostained with antibodies against ACTA2 or DES. As shown in Fig. 2B, both GFP+ and GFP− HSCs expressed ACTA2 or DES at day 7 in culture. A negative control without first antibodies did not show signal (Fig. 2C) and HSCs from MesP1$^{+/+}$;R26T/G$^{f/f}$ liver did not show GFP expression (Fig. 2D). These results demonstrate that HSCs are mesodermal in origin and are capable of differentiating into ACTA2+ myofibroblasts.

Activation of mesodermal HSCs in culture

We noted that there were GFP− HSCs in the MesP1$^{Cre/+}$;R26T/G$^{f/f}$ liver. To quantify GFP+ HSCs in the MesP1$^{Cre/+}$;R26T/G$^{f/f}$ liver, we analyzed HSCs via FACS on the basis of GFP expression and storage of vitamin A (VitA) lipids. Combining the detection of VitA autofluorescence and GFP using 350 (FL5) and 530 nm (FL1) filters, we separated the primary HSCs isolated from the MesP1$^{Cre/+}$;R26T/G$^{f/f}$ (Cre+) liver into VitA+GFP− or VitA+GFP+ fractions (Fig. 3A). FACS analysis revealed that approximately 70±9.4% (n=4) of VitA+ HSCs express GFP (Fig. 3A). The control MesP1$^{+/+}$;R26T/G$^{f/f}$ (Cre−) liver did not show GFP expression (Fig. 3A). We cultured HSCs isolated from the MesP1$^{Cre/+}$;R26T/G$^{f/f}$ liver for 13 days and performed another FACS analysis. As shown in Fig. 3B, the proportion of GFP+ HSCs remains the same (71%) in culture. These results indicate that at least 70% of HSCs derived from the MesP1+ mesoderm in the adult liver.

In general, the Cre-loxP system cannot achieve 100% recombination in mouse tissues due to insufficient amounts of Cre expression, DNA recombination, and partial inactivity of the promoter at the Rosa26 gene locus. Nevertheless, our results suggest that 30% of HSCs arise from origin(s) other than the MesP1+ mesoderm. To determine whether the GFP+ and GFP− HSCs have different characteristics, we sorted the VitA+GFP+ and VitA+GFP− HSCs from the primary (day 0) or culture activated HSCs (day 13) via FACS and compared their gene expression by QPCR (Fig. 3C,D). After isolation of HSCs by collagenase perfusion and discontinuous centrifugation, approximately 95% of the cells exhibited autofluorescence of VitA. The primary HSCs before FACS expressed HSC markers such as Des and Col1a1 (Fig. 3C, lane 1). QPCR detected inevitable contamination of hepatocytes (Alb), endothelial cells (Cd31), and Kupffer cells (Cd68) in the primary HSCs before FACS (Fig. 3D, lane 1). After sorting HSCs into VitA+GFP+ and VitA+GFP− fractions, the expression of these markers became undetectable (Fig. 3D, lanes 2,3), which confirmed the successful purification of HSCs. These genes were also undetectable in the day-13 HSCs (Fig. 3D, lane 4), suggesting that contaminating non-HSCs do not survive in culture.

The sorted VitA+GFP+ and VitA+GFP− HSCs from primary HSCs showed similar levels of Des, Col1a1, Timp1, Hgf, and Tgfb1 expression (Fig. 3C, lanes 2 and 3). Upon activation in culture, primary HSCs showed increased expression of activation markers (Acta2, Col1a1, and Timp1) when not subjected to FACS (Fig. 3B, lanes 1 and 4), while both VitA+GFP+ and VitA+GFP− HSCs from day-13 HSCs showed similar increases in these genes (lanes 5

and 6). This result suggests that the both GFP+ and GFP− HSCs have a similar phenotype in the normal liver and upon activation in vitro.

No contribution of HSCs and PFs to hepatocytes and cholangiocytes in liver fibrosis

Given that the MesP1$^{Cre/+}$;R26T/G$^{f/f}$ mouse labels 70% of liver mesenchymal cells in the adult liver, we tested whether the MesP1+ mesoderm-derived mesenchymal cells undergo MET and differentiate into hepatocytes and cholangiocytes in liver fibrosis. Following 30 CCl_4 injections, mouse livers developed fibrosis around the central vein. GFP expression was observed in mesenchymal cells in fibrotic septa or sinusoids and did not overlap with TOMATO+ hepatocytes (Fig. 4A). Immunohistochemistry confirmed that ACTA2+ DES+ myofibroblasts co-express GFP (80.0±3.6%, 2,590 ACTA2+ myofibroblasts examined, n=3); however, no GFP expression was observed in HNF4+ hepatocytes and CK19+ cholangiocytes (Fig. 4D,E).

We also analyzed the differentiation potential of the mesenchymal cells in biliary fibrosis. Two weeks after BDL, no GFP expression was observed in TOMATO+ cholangiocytes and hepatocytes (Fig. 4F). Immunohistochemistry showed that ACTA2+ myofibroblasts express GFP adjacent to the dilated bile duct (Fig. 4G, 79.3±4.0%, 2,865 ACTA2+ myofibroblasts examined, n=3). GFP expression was observed in DES+ myofibroblasts and activated HSCs in the sinusoid (Fig. 4H) but not in HNF4+ hepatocytes and CK19+ cholangiocytes (Fig. 4I,J). These data demonstrate that mesodermal mesenchymal cells, including HSCs and PFs, comprise a major source of myofibroblasts and do not undergo a MET during fibrogenesis to yield hepatocytes and cholangiocytes.

No contribution of HSCs and PFs to oval cells

Next, we challenged the notion that HSCs are progenitor cells for oval cells and give rise to hepatocytes and cholangiocytes via MET.[26,27] After inducing oval cells with a DDC diet for 4 weeks, GFP expression was observed in myofibroblasts adjacent to GFP− TOMATO+ oval cells (Fig. 5A). The immunohistochemistry of A6 antigen or EPCAM, markers for oval cells, confirmed no GFP expression in oval cells (Fig. 5B,C). We noted rare GFP+ cells embedded in oval cells, but these cells did not co-express EPCAM (Fig. 5C, double arrowheads). Oval cells expressing PROM1[35] did not express GFP (Fig. 5D). No GFP expression was observed in CK19+ cholangiocytes/oval cells and CDH1+ HNF4+ hepatocytes (Fig. 5E–G). GFP+ myofibroblasts were associated with GFP− oval cells and expressed ACTA2 (81.7±2.5%, 2,595 ACTA2+ myofibroblasts examined, n=3) or THY1 (Fig. 5I). The cell lineage tracing refutes the notion that HSCs undergo MET and differentiate into oval cells, cholangiocytes, and hepatocytes.

Following the induction of oval cells, we halted the DDC diet, fed the mice normal chow for 4 weeks, and determined whether GFP+ mesenchymal cells give rise to hepatocytes or cholangiocytes during recovery from injury. Termination of the DDC diet reduced the number of ACTA2+ myofibroblasts and oval cells expressing EPCAM (Supporting Fig. 2A–C). Although mesenchymal cells continued to express GFP, neither EPCAM+ CK19+ cholangiocytes nor CDH1+ HNF4+ hepatocytes were positive for GFP (Supporting Fig. 2C–F). Collectively, these data demonstrate that mesodermal mesenchymal cells, including

HSCs and PFs, do not contribute to oval cells, hepatocytes, and cholangiocytes in mouse liver injury.

Discussion

The present study demonstrates that HSCs derive from the MesP1+ mesoderm in the adult liver. Our data demonstrate that this mesoderm population contributes to HSCs but not to endodermal cells, such as hepatocytes and cholangiocytes, in the adult liver. Given that MesP1 is transiently expressed during gastrulation, and not expressed in the developing and adult liver, our data indicate that no differentiation of HSCs to endodermal epithelial cells occurs during or after liver development.

We previously found that MCs migrate inward from the liver surface and give rise to HSCs, fibroblasts around the vein, and SMCs during liver development.[11] In contrast, MCs did not differentiate into liver epithelial cells. In agreement with this notion, the present study found that fibroblasts around the portal vein and SMCs in the portal vein are derived from the MesP1+ mesoderm similar to HSCs. We defined these fibroblasts around the portal vein as PFs based on expression of ELN, a marker for rat PFs, and DES. However, PFs isolated from rat liver are known to be negative for DES.[34] It remains elusive whether marker expression in fibroblasts around the portal vein is different among species or heterogeneous fibroblasts exist in the connective tissue. In the BDL model using the MesP1^{Cre};R26T/G^{f} mouse, GFP+ myofibroblasts accumulated around the bile duct in the portal area and no GFP+ cholangiocytes and hepatocytes were found, indicating that PFs are the primary source of myofibroblasts and that no MET occurs during biliary fibrosis. Similar to the BDL model, CCl_4-induced liver fibrosis did not provoke MET from MesP1+ mesoderm-derived HSCs to hepatocytes and cholangiocytes in the MesP1^{Cre};R26T/G^{f} mouse. In conclusion, our study did not find evidence of mesodermal mesenchymal cells undergoing MET to become hepatocytes or cholangiocytes during liver fibrosis.

Contrary to our conclusion, Yang et al. reported that HSCs give rise to oval cells using the GFAP^{Cre} and Rosa26YFP reporter mice.[26] These authors traced HSCs based on the expression of GFAP, which is a marker for HSCs in rats and humans. However, in mice, both HSCs and cholangiocytes express GFAP. Given that cholangiocytes are likely to be the origin of oval cells, the GFAP^{Cre} mouse would label cholangiocyte-derived oval cells in addition to HSCs. Thus, the GFAP^{Cre} mouse is not appropriate for tracing HSC lineages. The same group also reported differentiation of myofibroblasts to hepatocytes and cholangiocytes in the BDL model.[27] After BDL, they labeled activated HSCs by tamoxifen using the ACTA^{CreERT2} and Rosa26YFP^{flox} mouse and subsequently found YFP+ liver epithelial cells. In contrast to their findings, our study did not show such transdifferentiation from HSCs to liver epithelial cells in the BDL model in the MesP1^{Cre};R26T/G^{flox} mice. One possible reason for this discrepancy is that the BDL surgery on the ACTA^{CreERT2} mouse may activate de novo expression of Acta2 mRNA in epithelial cells, thereby inducing YFP expression upon tamoxifen injection in Acta2-expressing epithelial cells independent of HSC transdifferentiation. In fact, the same group reported induction of ACTA2 expression in hepatocytes and cholangiocytes.[13,26] Similar to our conclusion, no MET from HSCs to liver epithelial cells was observed in CCl_4-induced fibrosis using Collagen1a2^{Cre} and

Vimentin^{CreERT2} mice.[6,15] Mederacke et al. generated a HSC-specific lecithin-retinol acyltransferase (Lrat) Cre mouse line, which efficiently marks 99% of HSCs in the mouse liver.[36] Using this mouse, they reached the same conclusion that HSCs are the major source of myofibroblasts and do not give rise to oval cells, hepatocytes, and cholangiocytes. An important addition of our study using the MesP1^{Cre} mouse is that we demonstrated at least 70% of HSCs are derived from MesP1+ mesoderm and they do not differentiate into endodermal epithelial cells throughout liver development, growth, injury, and regeneration. We conclude that mesodermal liver mesenchymal cells are the primary source of myofibroblasts and do not undergo MET in vivo to yield oval cells or other liver epithelial cell types.

We found that 70% of HSCs express GFP in the MesP1^{Cre};R26T/G^{f} mouse liver. It is unclear why not all HSCs express GFP in this model, but inefficiency of DNA recombination by Cre or silencing of the CAG promoter in the Rosa26 locus may have attributed to the generation of GFP− HSCs in the liver. Another possible explanation is that the GFP− HSCs originated from other sources than the MesP1+ mesoderm. Although we cannot identify the origin of the GFP− HSCs in this model, we did not observe differences between GFP+ and GFP− HSCs in the MesP1^{Cre};R26T/G^{f} mouse in morphology or gene expression in either the quiescent or activated state. MesP1 expression was restricted to the portion of the mesoderm ingressed through the primitive streak in early embryos.[30] Therefore, GFP− HSCs might have originated from the MesP1− mesoderm adjacent to the MesP1+ mesoderm area.

HSCs have been known to exhibit multipotency in culture.[28,29] However, we have not been able to detect the transdifferentiation of HSCs in embryonic or adult livers. As demonstrated by direct cell reprogramming with defined factors in vitro,[37] in vitro culture environments might change gene expression and chromatin state of HSCs and negate the negative regulation that inhibits the multi-differentiation potential of HSCs in vivo. Although HSCs can differentiate into hepatocytes in vitro, our study indicates that the in vivo environments are not permissive for HSCs to alter their programmed lineage to differentiate into other germ layers. Our data indicate that the fate of liver mesenchymal cells is tightly regulated in vivo.

Myofibroblasts synthesize proinflammatory cytokines and extracellular matrices and participate in liver fibrosis. Our studies determined that liver mesenchymal cells are the major source of myofibroblasts. Specific targeting of HSCs, PFs, or MCs will be an important issue for the suppression of fibrosis and its progression to cirrhosis.

Supplementary Material

Refer to Web version on PubMed Central for supplementary material.

Acknowledgments

The authors thank Henry Sucov for providing the MesP1^{Cre} mouse and Yuchang Li, Nirmala Mavila and Sarah Utley for their assistance with the mouse models.

Financial Support

This work was supported by NIH grant R01AA020753 (to K.A.), pilot project funding (to K.A.) from P50AA011999, pilot project funding (to K.A.) from P30DK048522, and training program (to I.L.) from T32HD060549.

List of Abbreviations

ACTA2	α-smooth muscle actin
BDL	bile duct ligation
CDH1	E-cadherin
CK19	cytokeratin 19
CreERT2	Cre recombinase fused to a mutated ligand-binding domain of the human estrogen receptor
DDC	3,5-diethoxycarbonyl-1,4-dihydrocollidine
DES	DESMIN
ELN	elastin
EMT	epithelial-mesenchymal transition
FACS	fluorescence-activated cell sorting
GFAP	glial fibrillary acidic protein
GFP	green fluorescence protein
HSCs	hepatic stellate cells
MCs	mesothelial cells
MesP1	mesoderm posterior 1
MET	mesenchymal-epithelial transition
QPCR	quantitative PCR
PDPN	podoplanin
PFs	portal fibroblasts
PROM1	promin 1/CD133
R26T/G^{f}	Rosa26mTmG^{flox}
SMCs	smooth muscle cells
VitA	vitamin A

References

1. Iredale JP. Models of liver fibrosis: exploring the dynamic nature of inflammation and repair in a solid organ. J Clin Invest. 2007; 117:539–548. [PubMed: 17332881]
2. Friedman SL. Mechanisms of hepatic fibrogenesis. Gastroenterology. 2008; 134:1655–1669. [PubMed: 18471545]
3. Pinzani M, Macias-Barragan J. Update on the pathophysiology of liver fibrosis. Expert Rev Gastroenterol Hepatol. 2010; 4:459–472. [PubMed: 20678019]

4. Kisseleva T, Brenner DA. Anti-fibrogenic strategies and the regression of fibrosis. Best Pract Res Clin Gastroenterol. 2011; 25:305–317. [PubMed: 21497747]
5. Kisseleva T, Cong M, Paik Y, Scholten D, Jiang C, Benner C, et al. Myofibroblasts revert to an inactive phenotype during regression of liver fibrosis. Proc Natl Acad Sci U S A. 2012; 109:9448–9453. [PubMed: 22566629]
6. Troeger JS, Mederacke I, Gwak GY, Dapito DH, Mu X, Hsu CC, et al. Deactivation of hepatic stellate cells during liver fibrosis resolution in mice. Gastroenterology. 2012; 143:1073–1083. [PubMed: 22750464]
7. Zhang DY, Friedman SL. Fibrosis-dependent mechanisms of hepatocarcinogenesis. Hepatology. 2012; 56:769–775. [PubMed: 22378017]
8. Dranoff JA, Wells RG. Portal fibroblasts: Underappreciated mediators of biliary fibrosis. Hepatology. 2010; 51:1438–1444. [PubMed: 20209607]
9. Li Y, Wang J, Asahina K. Mesothelial cells give rise to hepatic stellate cells and myofibroblasts via mesothelial-mesenchymal transition in liver injury. Proc Natl Acad Sci U S A. 2013; 110:2324–2329. [PubMed: 23345421]
10. Asahina K, Tsai SY, Li P, Ishii M, Maxson RE Jr, Sucov HM, et al. Mesenchymal origin of hepatic stellate cells, submesothelial cells, and perivascular mesenchymal cells during mouse liver development. Hepatology. 2009; 49:998–1011. [PubMed: 19085956]
11. Asahina K, Zhou B, Pu WT, Tsukamoto H. Septum transversum-derived mesothelium gives rise to hepatic stellate cells and perivascular mesenchymal cells in developing mouse liver. Hepatology. 2011; 53:983–995. [PubMed: 21294146]
12. Zeisberg M, Yang C, Martino M, Duncan MB, Rieder F, Tanjore H, et al. Fibroblasts derive from hepatocytes in liver fibrosis via epithelial to mesenchymal transition. J Biol Chem. 2007; 282:23337–2347. [PubMed: 17562716]
13. Sicklick JK, Choi SS, Bustamante M, McCall SJ, Pérez EH, Huang J, et al. Evidence for epithelial-mesenchymal transitions in adult liver cells. Am J Physiol Gastrointest Liver Physiol. 2006; 291:G575–G583. [PubMed: 16710052]
14. Rygiel KA, Robertson H, Marshall HL, Pekalski M, Zhao L, Booth TA, et al. Epithelial-mesenchymal transition contributes to portal tract fibrogenesis during human chronic liver disease. Lab Invest. 2008; 88:112–123. [PubMed: 18059363]
15. Scholten D, Osterreicher CH, Scholten A, Iwaisako K, Gu G, Brenner DA, et al. Genetic labeling does not detect epithelial-to-mesenchymal transition of cholangiocytes in liver fibrosis in mice. Gastroenterology. 2010; 139:987–998. [PubMed: 20546735]
16. Chu AS, Diaz R, Hui JJ, Yanger K, Zong Y, Alpini G, et al. Lineage tracing demonstrates no evidence of cholangiocyte epithelial-to-mesenchymal transition in murine models of hepatic fibrosis. Hepatology. 2011; 53:1685–1695. [PubMed: 21520179]
17. Si-Tayeb K, Lemaigre FP, Duncan SA. Organogenesis and development of the liver. Dev Cell. 2010; 18:175–189. [PubMed: 20159590]
18. Carpentier R, Suñer RE, van Hul N, Kopp JL, Beaudry JB, Cordi S, et al. Embryonic ductal plate cells give rise to cholangiocytes, periportal hepatocytes, and adult liver progenitor cells. Gastroenterology. 2011; 141:1432–1438. [PubMed: 21708104]
19. Farber E. Similarities in the sequence of early histological changes induced in the liver of the rat by ethionine, 2-acetylamino-fluorene, and 3'-methyl-4-dimethylaminoazobenzene. Cancer Res. 1956; 16:142–148. [PubMed: 13293655]
20. Duncan AW, Dorrell C, Grompe M. Stem cells and liver regeneration. Gastroenterology. 2009; 137:466–481. [PubMed: 19470389]
21. Yanger K, Stanger BZ. Facultative stem cells in liver and pancreas: fact and fancy. Dev Dyn. 2011; 240:521–529. [PubMed: 21312313]
22. Boulter L, Lu WY, Forbes SJ. Differentiation of progenitors in the liver: a matter of local choice. J Clin Invest. 2013; 123:1867–1873. [PubMed: 23635784]
23. Okabe M, Tsukahara Y, Tanaka M, Suzuki K, Saito S, Kamiya Y, et al. Potential hepatic stem cells reside in EpCAM+ cells of normal and injured mouse liver. Development. 2009; 136:1951–1960. [PubMed: 19429791]

24. Español-Suñer R, Carpentier R, Van Hul N, Legry V, Achouri Y, Cordi S, et al. Liver progenitor cells yield functional hepatocytes in response to chronic liver injury in mice. Gastroenterology. 2012; 143:1564–1575. [PubMed: 22922013]
25. Paku S, Schnur J, Nagy P, Thorgeirsson SS. Origin and structural evolution of the early proliferating oval cells in rat liver. Am J Pathol. 2001; 158:1313–1323. [PubMed: 11290549]
26. Yang L, Jung Y, Omenetti A, Witek RP, Choi S, Vandongen HM, et al. Fate-mapping evidence that hepatic stellate cells are epithelial progenitors in adult mouse livers. Stem Cells. 2008; 26:2104–2113. [PubMed: 18511600]
27. Michelotti GA, Xie G, Swiderska M, Choi SS, Karaca G, Krüger L, et al. Smoothened is a master regulator of adult liver repair. J Clin Invest. 2013; 123:2380–2394. [PubMed: 23563311]
28. Kordes C, Sawitza I, Müller-Marbach A, Ale-Agha N, Keitel V, Klonowski-Stumpe H, et al. CD133+ hepatic stellate cells are progenitor cells. Biochem Biophys Res Commun. 2007; 352:410–417. [PubMed: 17118341]
29. Conigliaro A, Amicone L, Costa V, De Santis Puzzonia M, Mancone C, Sacchetti B, et al. Evidence for a common progenitor of epithelial and mesenchymal components of the liver. Cell Death Differ. 2013; 20:1116–1123. [PubMed: 23686136]
30. Saga Y, Kitajima S, Miyagawa-Tomita S. Mesp1 expression is the earliest sign of cardiovascular development. Trends Cardiovasc Med. 2000; 10:345–352. [PubMed: 11369261]
31. Muzumdar MD, Tasic B, Miyamichi K, Li L, Luo L. A global double-fluorescent Cre reporter mouse. Genesis. 2007; 45:593–605. [PubMed: 17868096]
32. Preisegger KH, Factor VM, Fuchsbichler A, Stumptner C, Denk H, Thorgeirsson SS. Atypical ductular proliferation and its inhibition by transforming growth factor beta1 in the 3,5-diethoxycarbonyl-1,4-dihydrocollidine mouse model for chronic alcoholic liver disease. Lab Invest. 1999; 79:103–109. [PubMed: 10068199]
33. Engelhardt NV, Factor VM, Yasova AK, Poltoranina VS, Baranov VN, Lasareva MN. Common antigens of mouse oval and biliary epithelial cells. Expression on newly formed hepatocytes. Differentiation. 1990; 45:29–37. [PubMed: 2292360]
34. Li Z, Dranoff JA, Chan EP, Uemura M, Sévigny J, Wells RG. Transforming growth factor-β and substrate stiffness regulate portal fibroblast activation in culture. Hepatology. 2007; 46:1246–1256. [PubMed: 17625791]
35. Rountree CB, Barsky L, Ge S, Zhu J, Senadheera S, Crooks GM. A CD133-expressing murine liver oval cell population with bilineage potential. Stem Cells. 2007; 25:2419–2429. [PubMed: 17585168]
36. Mederacke I, Hsu CC, Troeger JS, Huebener P, Mu X, Dapito DH, et al. Fate tracing reveals hepatic stellate cells as dominant contributors to liver fibrosis independent of its aetiology. Nat Commun. 2013; 4:2823. [PubMed: 24264436]
37. Aoi T, Yae K, Nakagawa M, Ichisaka T, Okita K, Takahashi K, et al. Generation of pluripotent stem cells from adult mouse liver and stomach cells. Science. 2008; 321:699–702. [PubMed: 18276851]

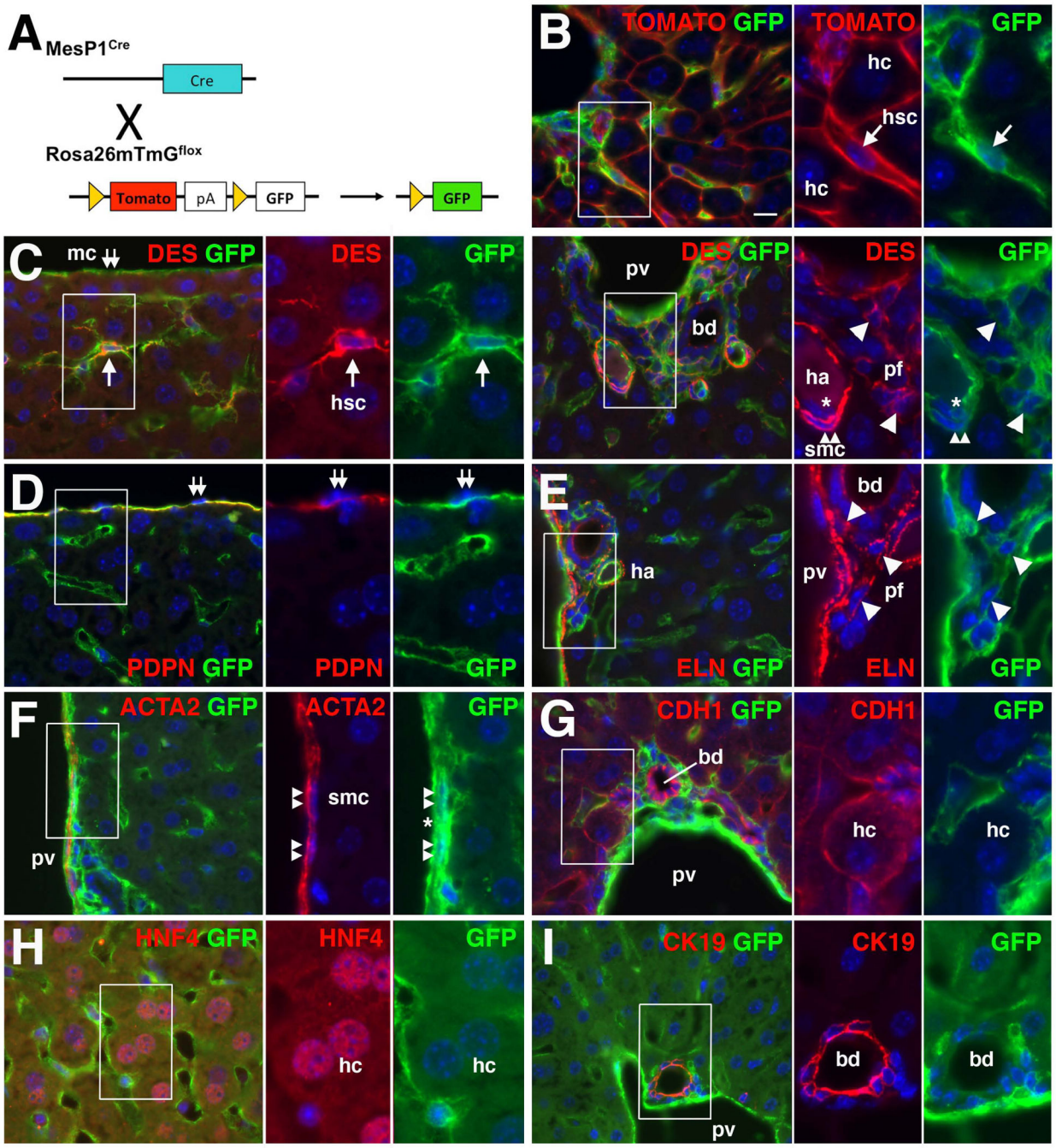

Fig. 1.

Contribution of MesP1+ mesoderm to HSCs, PFs, SMCs, and MCs, but not hepatocytes and cholangiocytes, in the adult liver. (A) A cell lineage analysis using the MesP1^{Cre} and R26T/G^{flox} mice. (B) Expression of TOMATO and GFP in the MesP1$^{Cre/+}$;R26T/G$^{f/f}$ adult liver. Membrane-tagged TOMATO and GFP are observed in hepatocytes (hc) and HSCs (hsc) in the sinusoid, respectively. No GFP expression in hepatocytes (2,000 hepatocytes examined, n=3 mice). (C–I) Immunohistochemistry of the adult MesP1$^{Cre/+}$;R26T/G$^{f/f}$ mouse liver for GFP with DES (C), PDPN (D), ELN (E), ACTA2 (F), CDH1 (G), HNF4

(H), or CK19 (I). Arrows indicate GFP+ HSCs in the sinusoid. Arrowheads and double arrows indicate DES+ ELN+ PFs adjacent to the bile duct (bd) and GFP+ MCs on the liver surface, respectively. Double arrowheads indicate DES+ ACTA2+ SMCs in the portal vein (pv) and hepatic artery (ha). GFP+ endothelial cells in the portal vein and hepatic artery are indicated by asterisks. No GFP expression in CDH+ HNF4+ hepatocytes and CDH+ CK19+ cholangiocytes (2,049 CDH1+, 1,836 HNF4+ hepatocytes and 1,036 CDH1+, 1,093 CK19+ cholangiocytes examined, n=3). Nuclei were counterstained with DAPI. Scale bar is 10 μm.

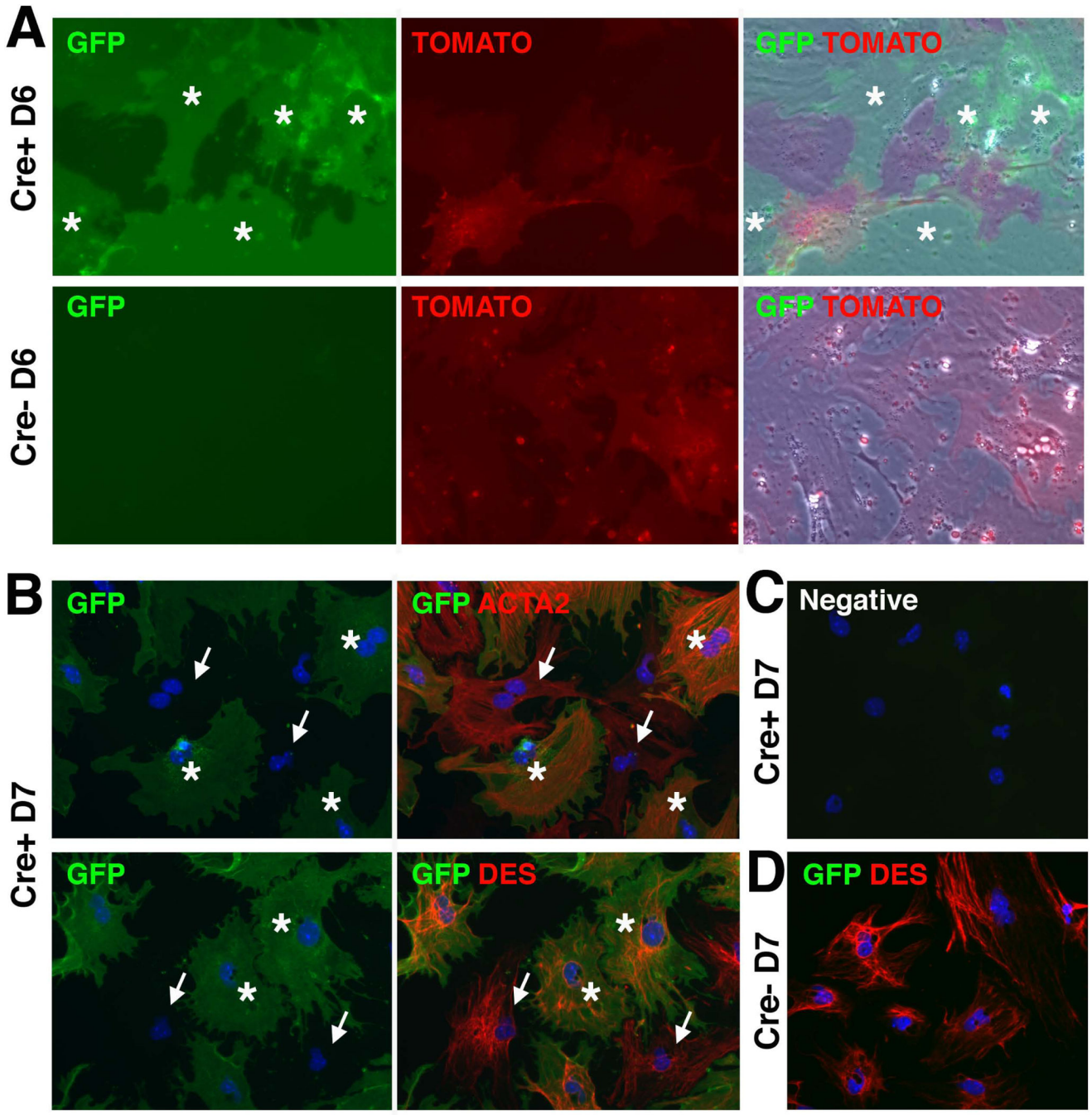

Fig. 2.

In vitro activation of mesodermal HSCs. HSCs were isolated from the normal MesP1$^{Cre/+}$ or MesP1^{++};R26T/G$^{f/f}$ adult livers and were cultured for 6 (A) and 7 days (B–D). (A) Expression of TOMATO and GFP in HSCs. Asterisks indicate GFP+ HSCs isolated from the MesP1$^{Cre/+}$;R26T/G$^{f/f}$ adult liver (Cre+). No GFP expression in HSCs from the MesP1^{++};R26T/G$^{f/f}$ liver (Cre−). (B) Immunostaining of GFP and ACTA2 or DES in HSCs isolated from the MesP1$^{Cre/+}$;R26T/G$^{f/f}$ adult liver (Cre+). Asterisks indicate GFP+ HSCs expressing ACTA2 or DES. Arrows indicate GFP− HSCs expressing ACTA2 or DES. (C) A

negative control without primary antibodies. (D) Immunostaining of GFP and DES. No GFP expression in HSCs isolated from the MesP1^{++};R26T/G$^{f/f}$ liver (Cre−). Nuclei were counterstained with DAPI.

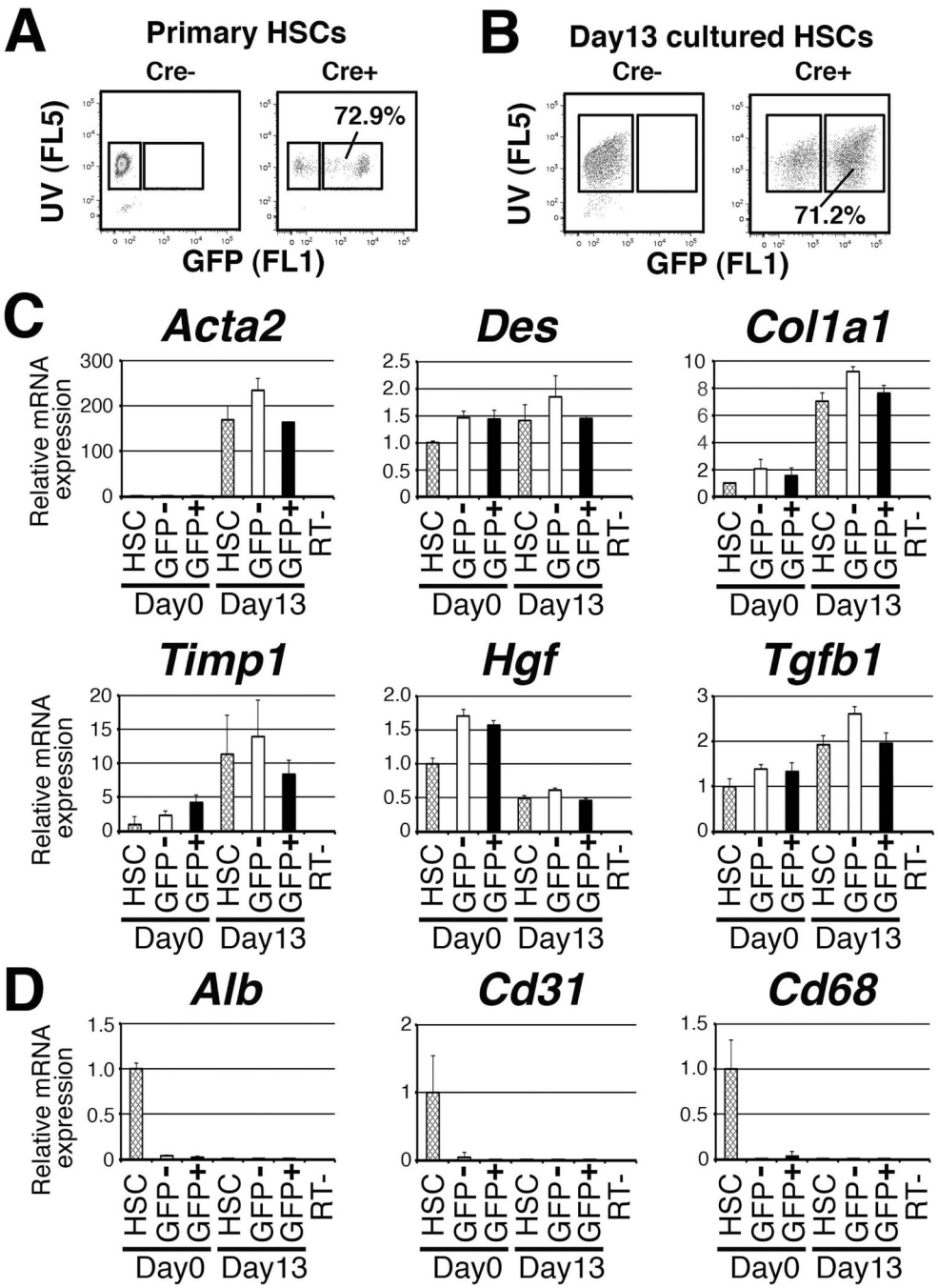

Fig. 3.

Similar phenotypes of GFP+ and GFP− HSCs in the MesP1$^{Cre/+}$;R26T/G$^{f/f}$ liver. (A) HSCs were isolated from the MesP1$^{Cre/+}$;R26T/G$^{f/f}$ (Cre+) or MesP1$^{+/+}$;R26T/G$^{f/f}$ (Cre−) livers and were subjected to FACS. HSCs were analyzed by storage of VitA (FL5) and expression of GFP (FL1). (B) HSCs were isolated from the Cre+ and Cre− mice, cultured for 13 days, and subjected to FACS analysis. (C,D) HSCs were isolated from the MesP1$^{Cre/+}$;R26T/G$^{f/f}$ liver and the primary (day 0) and cultured HSCs (day 13) were subjected to QPCR. In addition, VitA+GFP+ and VitA+GFP− HSCs sorted from the primary or day-13 HSCs were

also subjected to QPCR for measurement for HSC markers (C) and other liver cell types (D). The results are expressed as relative expression compared against primary HSCs (day 0). The values were normalized against Gapdh. Each value is the mean ± standard deviation of the triplicate measurements.

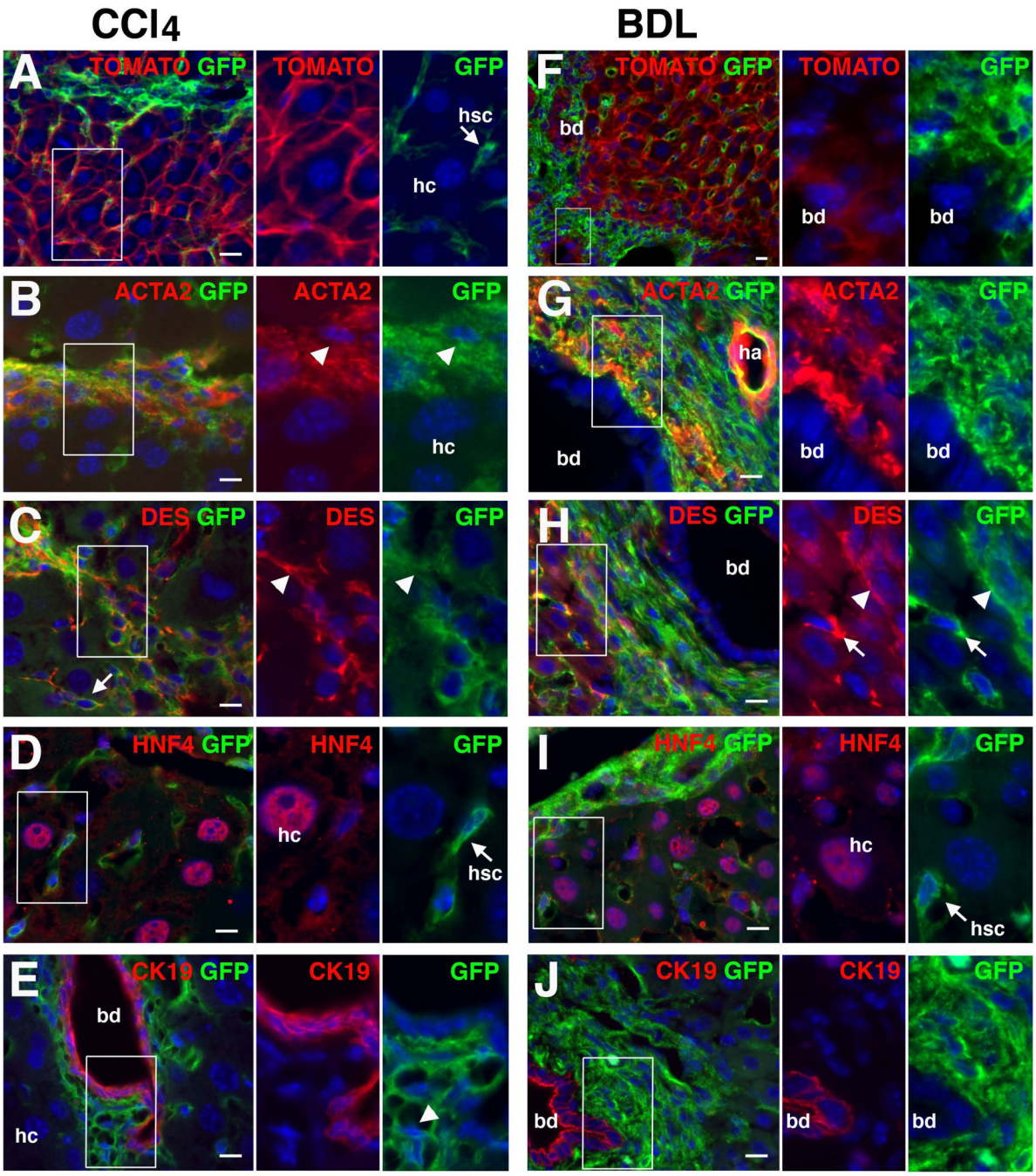

Fig. 4.

No contribution of mesodermal mesenchymal cells to hepatocytes and cholangiocytes in liver fibrosis. Lineage of mesodermal mesenchymal cells was traced using the MesP1$^{Cre/+}$;R26T/G$^{f/f}$ mouse in liver fibrosis induced by CCl_4 injections 30 times (A–E) or by BDL for 2 weeks (F–J). (A,F) Expression of TOMATO and GFP in the liver. No GFP expression in TOMATO+ hepatocytes (hc) and cholangiocytes (bd). An arrow indicates GFP+ HSCs in the sinusoid. (B–E) Immunohistochemistry of the CCl_4-induced fibrotic livers with antibodies against GFP and ACTA2 (B), DES (C), HNF4 (D), or CK19 (E). GFP

is expressed in ACTA2+ DES+ myofibroblasts (arrowheads) and DES+ activated HSCs in the sinusoid (arrows) but not in HNF4+ hepatocytes and CK19+ cholangiocytes (1,645 hepatocytes and 1,322 cholangiocytes examined, n=3 mice). (G-J) Immunohistochemistry of the BDL-induced fibrotic livers with antibodies against GFP and ACTA2 (G), DES (H), HNF4 (I), or CK19 (J). GFP is expressed in ACTA2+ DES+ myofibroblasts (arrowheads) and DES+ activated HSCs in the sinusoid (arrows) but not in HNF4+ hepatocytes and CK19+ cholangiocytes (1,852 hepatocytes and 2,560 cholangiocytes examined, n=3). Nuclei were counterstained with DAPI. Scale bars are 10 μm.

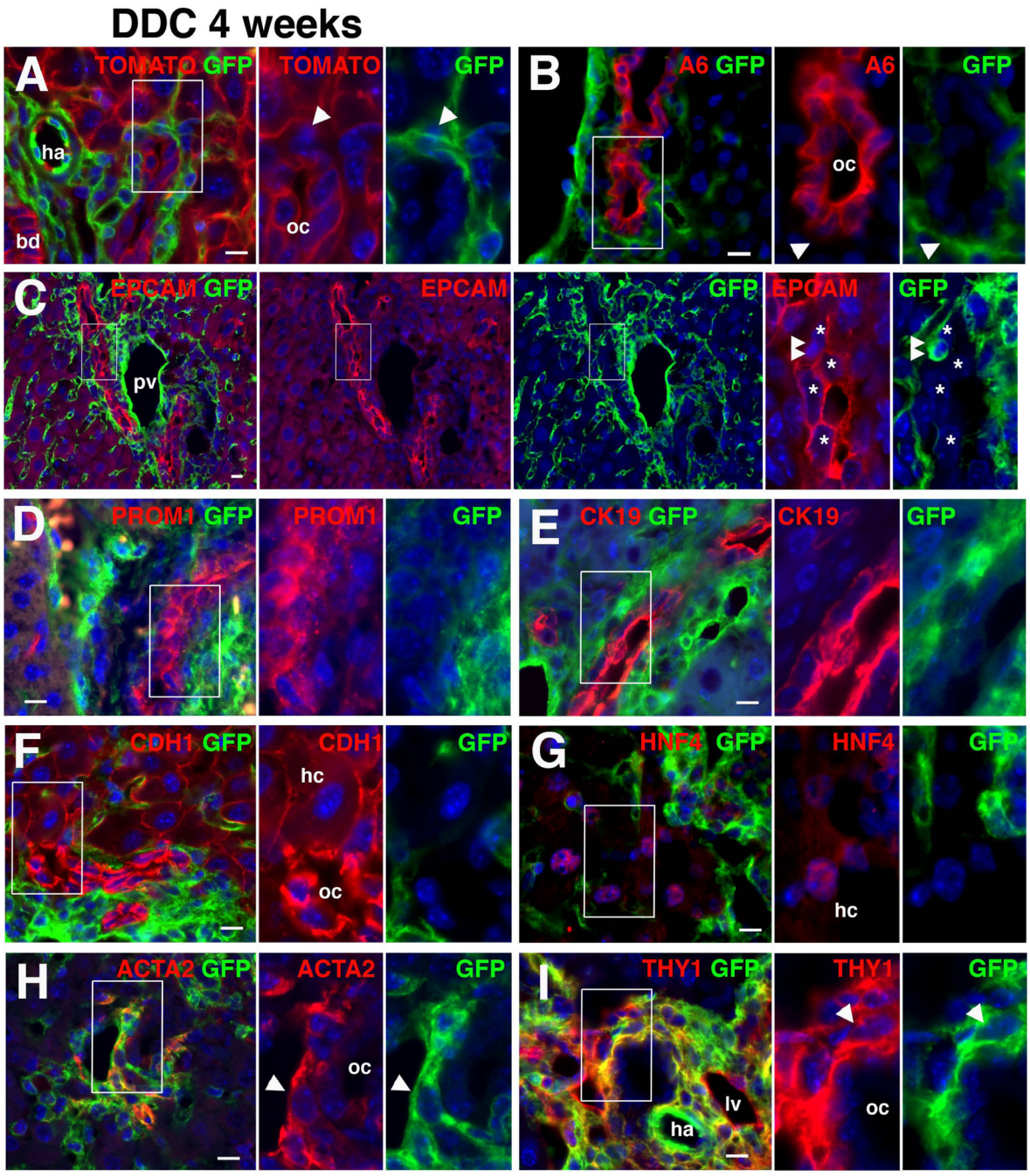

Fig. 5.

No contribution of mesodermal mesenchymal cells to oval cells, hepatocytes and cholangiocytes in injured liver. Lineage of mesodermal mesenchymal cells was traced using the MesP1$^{Cre/+}$;R26T/G$^{f/f}$ mouse in injured liver induced by DDC diet for 4 weeks. (A) Expression of TOMATO and GFP in the liver. No GFP expression in TOMATO+ oval cells (oc). Arrowheads indicate mesenchymal cells. bd, bile duct; ha, hepatic artery. (B–I) Immunohistochemistry of the injured liver with antibodies against GFP and A6 (B), EPCAM (C), PROM1 (D), CK19 (E), CDH1 (F), HNF4 (G), ACTA2 (H) or THY1 (I). (B–

D) No GFP expression in oval cells expressing A6 antigen, EPCAM, and PROM1 (1,899 EPCAM+ oval cells examined, n=3 mice). Arrowheads indicate GFP+ myofibroblasts associated with GFP− oval cells. Asterisks indicate EPCAM+ oval cells. Double arrows show rare GFP+ cells embedded in oval cells. pv, portal vein. (E–G) No GFP expression in CK19+ cholangiocytes/oval cells and CDH1+ hepatocytes (hc)/oval cells, and HNF4+ hepatocytes (2,102 CK19+ cells, 2,749 CDH1+ cells and 2,120 HNF4+ hepatocytes examined, n=3). (H,I) Myofibroblasts associated with GFPcells, and HNF4+ hepatocytes (2,102 CK19+ cells, 2,749 CDH1+ cells and 2,120 HNF4+ hepatocytes examined, n=3). (H,I) Myofibroblasts associated with GFP− oval cells co-express GFP with ACTA2 or THY1. lv, lymphatic vessel. Nuclei were counterstained with DAPI. Scale bars are 10 μm.